JOURNAL OF MATERIALS SCIENCE 37 (2002) 325–334

Anisotropic mechanical properties of oriented HAPEX™

M. BONNER, L. S. SAUNDERS, I. M. WARD
IRC in Polymer Science and Technology, University of Leeds, Leeds, LS2 9JT, UK
E-mail: i.m.ward@leeds.ac.uk

G. W. DAVIES, M. WANG‡, K. E. TANNER, W. BONFIELD
IRC in Biomedical Materials, Queen Mary and Westfield College, Mile End Road, London, E1 4NS, UK

A detailed study has been undertaken of the anisotropic mechanical behaviour of oriented hydroxyapatite reinforced polymer composite (HAPEX™). The oriented material was produced by hydrostatic extrusion of isotropic HAPEX™. It was found that the tensile and shear moduli and strengths of the oriented HAPEX™ are substantially increased compared with isotropic HAPEX™. In particular, the properties along the extrusion direction exceed the lower range of the properties of cortical bone, showing that the oriented HAPEX™ is suitable for use in skeletal major load bearing applications.

1. Introduction

Bone is a natural composite, consisting of a collagen matrix filled with a brittle, but relatively high modulus filler, hydroxyapatite. An artificial bone replacement material, HAPEX™, has been developed by Bonfield *et al*., which consists of an inert polyethylene matrix containing 40 volume% of bioactive synthetic hydroxyapatite filler and is readily incorporated as a skeletal implant [1–3]. However this composite has mechanical properties at the lower bounds for cortical bone [4], which limits the clinical application to minor load bearing situations, such as middle ear prostheses and maxillo-facial implants [5, 6].

It is obviously desirable to produce a version of HAPEX™ with increased mechanical properties to allow application as a skeletal implant in major load bearing situations. Previous work [7–9] has shown that orientation can be induced in HAPEX™ by hydrostatic extrusion, which increases the mechanical properties of the material in the orientation direction. In this paper the mechanical properties of hydrostatically extruded HAPEX™, both parallel and perpendicular to the orientation direction are reported.

2. Experimental methods

2.1. Materials

The materials used in this work were unfilled polyethylene and HAPEX™. The synthetic hydroxyapatite filler was P205 grade obtained from Plasma Biotal Ltd (Tideswell, Derbyshire, UK), with a particle size distribution as shown in Table I, where $d(0.5)$ is the median diameter of the particles and $d(0.1)$ and diameter $d(0.9)$ are the diameters at 10% and 90% of the distribution. The unfilled polyethylene is the same grade as that used in clinical grade HAPEX™, namely HM 4560 XP supplied by BP Chemicals Ltd, which is an ethylene hexene co-polymer with less than 1.5 butyl branches per 1000 carbon atoms in the backbone. The $\overline{M}_W$ is 225,000 and the $\overline{M}_N$ is 24,000.

2.2. Manufacture of HAPEX™ billets

HAPEX™ was manufactured at the IRC in Biomedical Materials and full details of the production are described elsewhere [3]. Briefly, hydroxyapatite and polyethylene were pre-mixed before being compounded in a twin screw extruder (Betol BTL405). The feed from the extruder was pelletised and the pellets were then processed in a centrifugal mill (Fritsch Pulverisette 14). This process took place in three stages, with successively smaller sieve sizes being used at each stage: 2 mm, 1 mm and 0.2 mm. Care was taken to ensure that the mill was allowed to cool between each batch of HAPEX™ processed to minimise oxidi-ation of the material. After processing all visible contaminants (oxidised polymer caused by localised excessive heating) were removed. The powder was then compression moulded into cylindrical moulds (Fig. 1).

2.3. Hydrostatic extrusion

Hydrostatic extrusion is a method for inducing orientation in a material by solid phase deformation, utilising hydrostatic pressure and has been used to deform

‡*Present Address*: Department of Materials, Nanyang Technical University, Singapore.

TABLE I Particle size distribution of hydroxyapatite powder (P205)

Grade	$d(0.1)/\mu$m	$d(0.5)/\mu$m	$d(0.9)/\mu$m
P 205	1.26	4.04	8.77

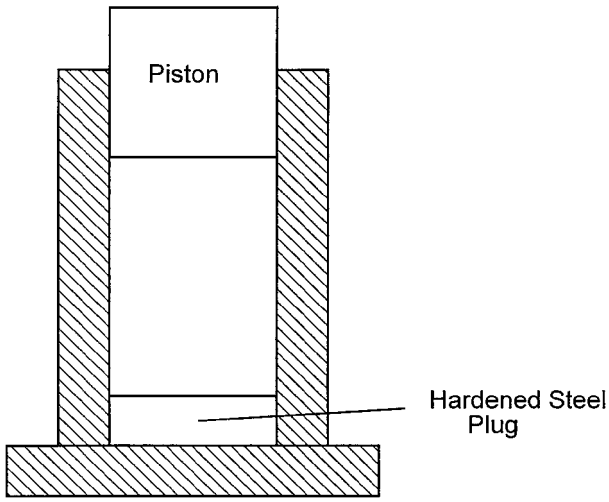

Figure 1 Schematic representation of a billet mould.

permanently such brittle materials as marble [10] and has been extensively used on metals [11] and a variety of polymers [12]. Hydrostatic extrusion uses back pressure to force a solid billet through a convergent die (Figs 2 and 3). In polymeric systems the billet is usually heated to an elevated temperature, which is high enough to allow flow, but below the melting point of the material. The pressure is provided by a fluid, which also lowers the friction between the billet and the die, enabling lower pressures to be used.

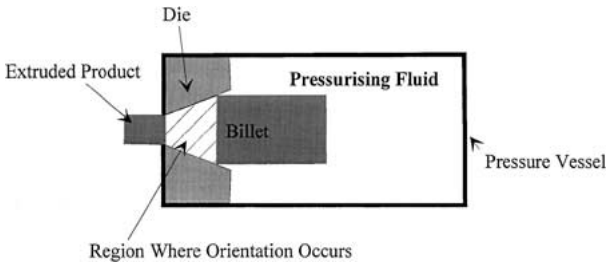

Figure 2 Schematic representation of a hydrostatic extruder.

Following previous work [7–9] the standard extrusion conditions used throughout this work for HAPEX^{TM} were a temperature of 115°C and an extrusion ratio (the ratio between the initial and final cross sectional areas) of 8:1. The standard extrusion conditions for unfilled polyethylene were a temperature of 100°C and an extrusion ratio of 8:1. The nominal diameters of the extruded product were 4 mm, 6 mm, 11 mm and 25 mm. Fig. 4 shows 4 mm and 25 mm diameter product. The extrusion pressure used varied depending upon the diameter of the final product. In all cases a polypropylene jacket as described in the next section was used to encase the billet and prevent the pressurising fluid making direct contact with the HAPEX^{TM} or polyethylene.

2.4. Polypropylene jackets

A major constraint on successful hydrostatic extrusion is the interaction between the billet material and the pressurising fluid. The use of a pressurising fluid which attacks the billet material can cause the material to stress crack, leading to an unusable end product [13]. Previous work [7–9] used two coats of a rubber based glue (Evostick®) to avoid direct contact with the pressurising fluid. While this method was partially successful, it was not sufficiently reproducible for commercial use. Thus, it was decided to enclose the HAPEX^{TM} billet in a sealed polypropylene jacket (Figs 5 and 6), enabling HAPEX^{TM} to be extruded under the same conditions, but with a slightly higher pressure and a success rate in excess of 95%.

2.5. Mechanical tests

2.5.1. Flexure

All flexural tests were performed on an Instron testing machine (at ambient temperature) in three point bending. Extruded material was tested as cylindrical rod,

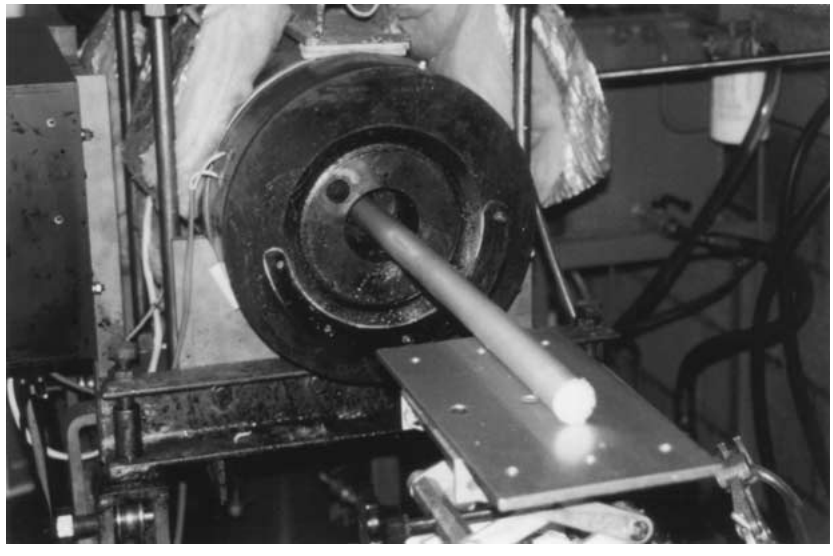

Figure 3 Extrusion apparatus showing 25 mm extrusion in progress.

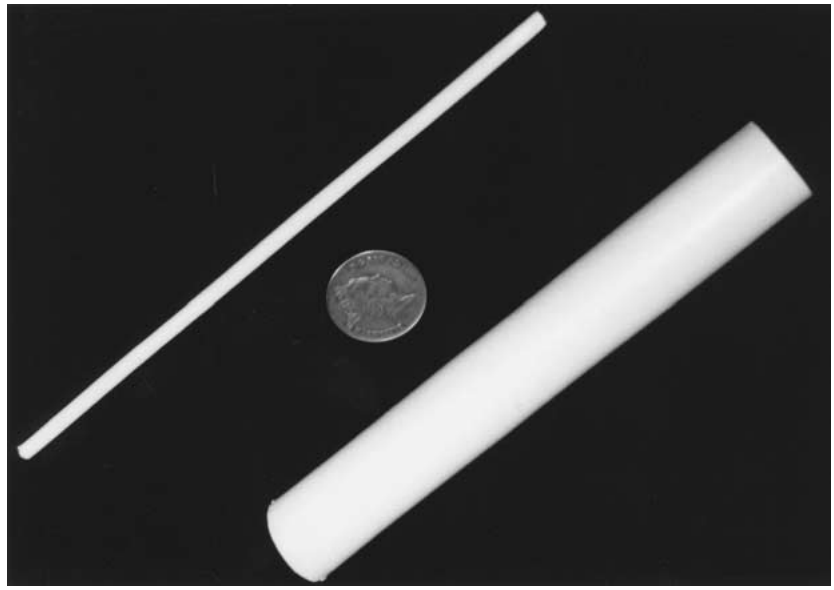

Figure 4 Extruded HAPEX^{TM} with 2p piece for scale.

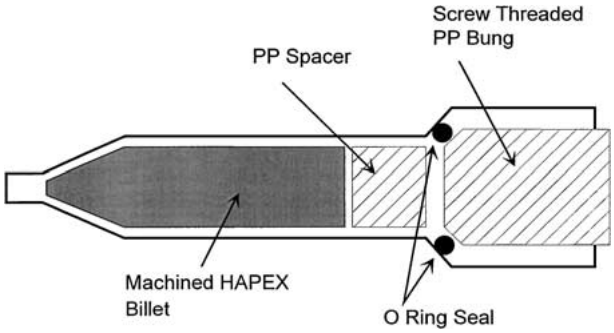

Figure 5 Schematic representation of the Polypropylene jacket and HAPEX^{TM} billet assembly.

while isotropic material was machined from rectangular compression moulded plates.

Two methods were used, a simple standard method, for initial characterisation and quality control, and a more sophisticated method, designed to obtain the ultimate modulus of the material, i.e. the modulus of the material at infinite span.

2.5.1.1. Method 1: Standard test. This test method was originally derived to cope with the small lengths and diameters of material that were produced during the initial trial phases of the extrusion process. However due to its speed and ease of use it was maintained as the main test for quality control and research purposes.

This method used spans (the distance between the supports) of 50 mm and 130 mm. At 50 mm span, the loading and support points were 10 mm diameter rods, while at 130 mm the supporting rods were 12.5 mm in diameter and the loading rod was 25 mm in diameter. The test samples were used "as is" for the 3.5 mm product, all other diameters were machined down to 3.5 mm diameter before testing. This gave aspect ratios of 14:1 at 50 mm span and 37:1 at 130 mm span. Flexural moduli at both spans were measured at the initial linear region of the stress strain curve, with due allowance for toe in, at a strain rate of 3.33×10^{-4} s^{-1}. Flexural strength was measured with a span of 50 mm, at a strain rate of 1.33×10^{-3} s^{-1} and the flexural strength was defined as the maximum stress developed in the material.

2.5.1.2. Method 2: Modulus at infinite span. This method was utilised after the introduction of the polypropylene jacket, when longer lengths of material became available.

This method used spans of 50, 100, 150 and 200 mm with samples machined to 3.5 mm diameter. In all cases the support and loading points were 10 mm diameter rods. Flexural modulus was measured in the initial linear region of the stress strain curve, with due allowance for toe in, at a crosshead speed which depended on the span being used (0.5 mm min^{-1}, 1 mm min^{-1}, 2 mm min^{-1}, 4 mm min^{-1} respectively). These crosshead speeds keep the strain rate within 10% of 3.33×10^{-4} s^{-1}. This method was used to predict the flexural modulus at infinite span, to eliminate the contribution of shear. This prediction was performed by plotting $\frac{1}{E}$ against $(\frac{\text{Diameter}}{\text{Span}})^2$ and extrapolating the curve to the y axis intercept, the intercept being the reciprocal of the modulus at infinite span. Since the limited nature of the data set means that it is impossible to say for certain exactly what trend the data are following, the simplest possible trend, a straight line, was used to perform the extrapolation.

2.5.2. Tensile tests

2.5.2.1. Extruded axial. The axial direction is defined as the direction of material orientation and the transverse direction is defined as perpendicular to the material orientation. Extruded material was tested as cylindrical rods.

The tests were performed on an RDP testing machine using an optical extensometer (RDP Howden Ltd), with software from Messphysik Laborgeräte GmbH to measure axial and transverse strain simultaneously. An

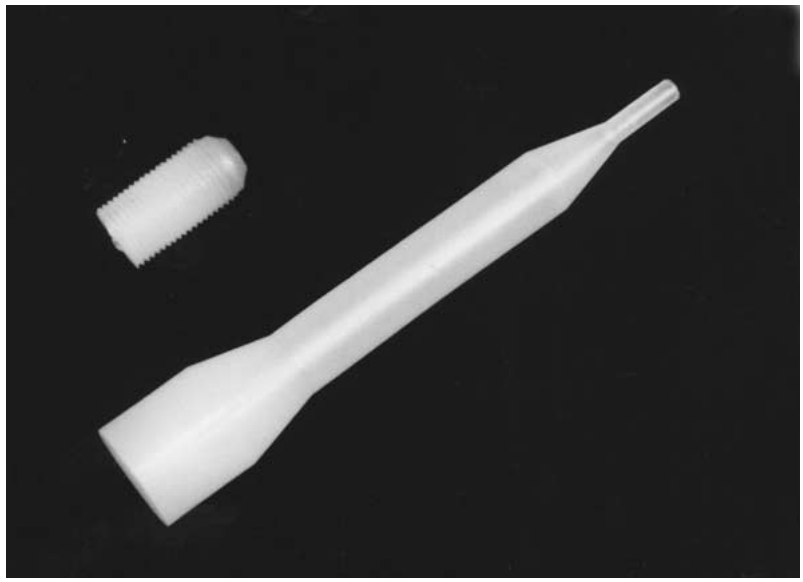

Figure 6 Polypropylene jacket assembly.

evenly illuminated white background was positioned behind the sample, so that the sample was in shadow and appeared as a black object to the extensometer, gave the best results with the least scatter. Small steel rods, 0.5 mm in diameter, were attached to the samples with small rubber O-rings to act as axial strain targets, while the sides of the sample were used as the transverse strain targets. Measuring axial and transverse strains simultaneously allowed the Poisson's ratio in the axial direction to be determined.

The sample gauge length was 100 mm, the diameter was 5 mm and the crosshead speed was 2 mm min^{-1}, giving a strain rate of 3.33×10^{-4} s^{-1}. The modulus was taken from the initial linear slope of the stress-strain curve, excluding the "toe-in" region.

2.5.2.2. Extruded transverse. These tests were performed using the same equipment as the axial tests, but the samples were too small to enable the use of the "shadow" technique. The samples were therefore illuminated from the front against a dark background, so that the sample appeared white. Black lines drawn on the sample using a fine tipped permanent OHP pen were used as strain targets. The sides of the sample were also used as targets to enable Poisson's ratio in the transverse direction to be measured. The samples were machined into rectangular bars, 5 mm wide, 2 mm deep and 16 mm long and the crosshead speed was 0.32 mm min^{-1}, giving a strain rate of 3.33×10^{-4} s^{-1}.

2.5.2.3. Isotropic. Isotropic material was tested in the form of bars machined from rectangular moulded plaques using the same testing techniques as for the axial extruded material. The samples were 100 mm long, 10 mm wide and 2 mm thick, the crosshead speed was 2 mm min^{-1}, giving a strain rate of 3.33×10^{-4} s^{-1}.

2.5.3. Torsion

Two methods were used to examine the torsional properties of the materials: a standard oscillating pendulum technique and a continuously driven technique.

2.5.3.1. Oscillating pendulum technique. The oscillating pendulum technique used machined rods 2.5 mm in diameter. The specimen was mounted vertically, with a fixed clamp at its lower end and a horizontal bar, with two steel masses, fixed to the upper end. The position of the steel masses on the bar could be altered to change the moment of inertia of the system. An angular transducer was attached to the bar and the output monitored by a data logger and analysed by a computer. The weight of the bar and transducer assembly was supported by a vertical wire to prevent an axial load being applied. The value of G, the torsional modulus was derived from the time period T using the equation:

$$G = \frac{2\omega^2 LI}{\pi r^4} = \frac{8\pi^2 LI}{\pi r^4 T^2} \quad (1)$$

where ω is the angular frequency, r is the specimen radius, L is the specimen length and I the moment of inertia of the bar. A range of specimen lengths was used to eliminate end effects and an average value of G reported once these end effects had become negligible.

2.5.3.2. Continuously driven technique. The continuously driven equipment was capable of several complete rotations enabling large strains to be applied. This equipment was simple, the sample being mounted vertically between two grips (Fig. 7 shows the torsion specimen sample geometry). The gripping arrangement used ball bearings in the grip mounts, making axial friction between the ball bearing and grip negligible, thus allowing the sample to change length during the test. The bottom grip was driven in continuous rotation by an electric stepper motor running through a reduction gear box and worm drive, allowing precise control of the rotation speed of the bottom grip. The upper grip was attached to a torque sensor, whose output was recorded by a computer. Rotational displacement was recorded by an optical disc sensor attached to the final worm drive. The sample geometry effectively negates end effects in the sample. The surface strain rate used was 0.004 s^{-1}.

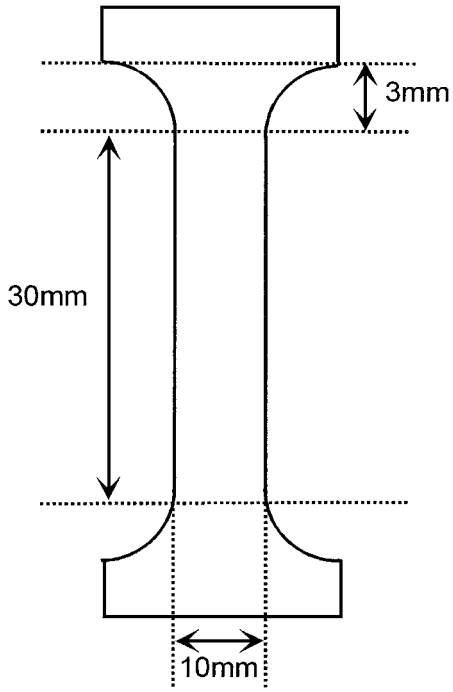

Figure 7 Diagram showing sample geometry for torsion specimens.

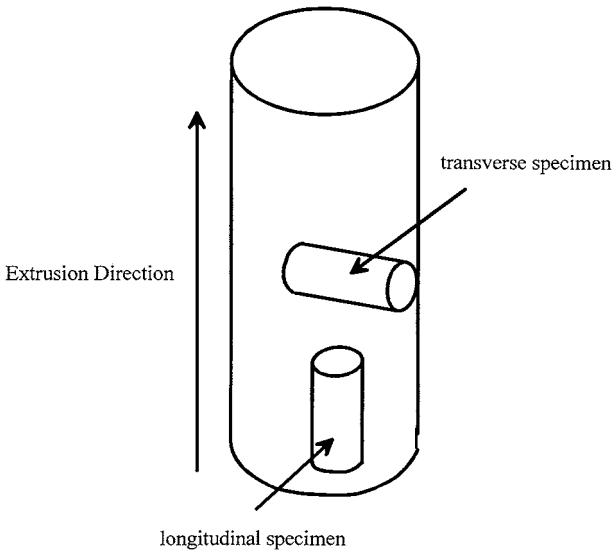

Figure 8 Diagram showing how compression test samples are cut from the extruded product.

The raw data were converted to stress-strain plots and corrected using the modified theory of Nadai [14].

2.5.4. Compression

Compression testing was performed in accordance with ASTM D 695M–85, except that, as the dimensions of the extruded specimens available were significantly smaller than the standard, the com-head speed was translated into a strain rate of 3.33×10^{-4} s^{-1}. Cylindrical specimens were 2.5 mm in diameter and 5 mm or 10 mm long to allow measurement of either yield point or modulus respectively, in accordance with ASTM D 695M-85. Extruded samples with diameters of 11 mm and 25 mm allowed specimens to be cut across the sample and hence the compressive properties of the material perpendicular to the extrusion direction could be measured (Fig. 8). The specimens were subjected to uniaxial compression and the displacement measured using an optical extensometer to monitor the compressive axial strain. The stress-strain curve was plotted and the gradient of the initial linear region measured, excluding the "toe-in" region. Isotropic samples were prepared in the same way, but the optical extensometer was not used.

2.5.5. Yield stress

There are several definitions of the yield point. The "classic" yield stress in a ductile material is the maximum stress reached before the material necks and draws. Another definition in oriented materials is a "knee" on the stress curve where there is a change in slope. However, in the isotropic materials studied here neither yield point was obvious, so an off-set value was chosen by considering the data obtained from the filled extruded material, which exhibited a yield point of the second type. First a line was drawn coincident with the initial gradient of the oriented material. This line was then shifted along the x-axis so that it passed through the yield point of the oriented material. The amount by which it needed to be shifted was converted to a percentage strain and this amount used as the off-set value for the isotropic materials. The off-set value used was equivalent to 2.11% strain. Although these definitions of the yield stress are arbitrary, they do allow a qualitative comparsion of the various materials.

3. Results

3.1. Modulus and strength

The flexural, tensile and compressive modulus and strength values for extruded and isotropic HAPEX^{TM} are shown in Table II. It can be seen that, as expected, the longer span flexural modulus, tensile modulus and compressive modulus are all consistent. The increase in the properties of the materials after hydrostatic extrusion is well demonstrated, with the isotropic material being relatively brittle, whereas the extruded material is ductile. Fig. 9 shows the marked differences in the tensile stress strain curves for isotropic and extruded materials.

There is also a significant increase in most of the material properties with the inclusion of the hydroxyapatite in the polyethylene. The exception to this trend is the tensile strength, where the greater ductility of the unfilled polyethylene allows the sample to reach high draw ratios with a consequent increase in the ultimate strength. The extremely ductile nature of the extruded materials in flexure should be emphasised. Flexural fracture of the extruded material is rare and large deformations can be achieved whilst maintaining sample integrity (Fig. 10).

3.2. Poisson's ratio

The initial Poisson's ratios for the materials are shown in Table III. The tests show some considerable noise at the start of the test, Fig. 11, and so the data in this region were averaged to produce a Poisson's ratio for each test. Both the mean of these "averages" and the

TABLE II Mechanical properties for isotropic and extruded polyethylene (PE) and HAPEX™

	Isotropic		Extruded	
	PE	HAPEX™	PE	HAPEX™
FM_{50} (GPa)	1.1	–	–	8.5
FM_{130} (GPa)		4.6 (4.4–5.1)	6.1 (5.7–6.1)	10.2
FM_{∞} (GPa)	–	–	–	10.2
TM_{AX} (GPa)	0.6	4.5 (3.8–5.0)	6.0	10.3 (9.5–11.0)
TM_{TR} (GPa)	–	–	–	5 (3.5–6.7)
CM_{AX} (GPa)	0.6	3.9	0.8 (0.5–1.1)	10 (7–13)
CM_{TR} (GPa)	–	–	1.2	5.3 (3.9–6.2)
FS (MPa)	23	29 (28–33)	50	85 (76–87)
Fε at failure (%)	Did not fail	1 (0.7–1.4)	Did Not Fail	
TS_{AX} (MPa)	15 (yield)	18 (15–20)	158	80 (75–84)
TS_{TR} (MPa)	–	–	–	9 (9–10)
Tε at failure (%)	>360	0.75 (0.5–0.9)		11 (10–12)
CS_{AX} (MPa)	16	40	25	36 (34–37)
CS_{TR} (MPa)	–	–	19 (18–20)	58 (58–59)

(F Flexural, T Tensile, C Compressive, M Modulus, S Strength, ε Strain, AX Axial, TR Transverse, 50 130 ∞ span in millimetres).

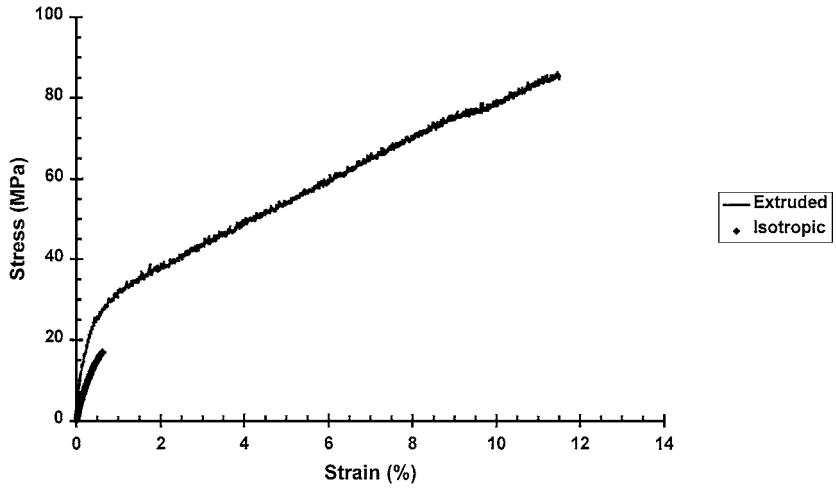

Figure 9 Tensile stress strain curves for extruded and isotropic HAPEX™.

TABLE III Poisson's ratios for isotropic and extruded HAPEX™

	Isotropic HAPEX™	Extruded HAPEX™
Axial	0.4 (0.38–0.43)	0.43 (0.4–0.45)
Transverse	–	0.4 (0.4–0.5)

range are quoted in Table III. There is a large amount of vibrational noise in the case of the transverse specimens, because the sample fails at extremely low strains, before the system has had a chance to settle.

3.3. Torsion

The torsional modulus and strength for the various materials tested are shown in Table IV, and Fig. 12 shows sample torsion plots.

Table IV clearly shown that the addition of the hydroxyapatite significantly increases the torsional modulus of the material, and this is further enhanced by hydrostatic extrusion. However as Fig. 12 also shows, the isotropic HAPEX™ is significantly more brittle than the extruded material.

TABLE IV Torsional properties for isotropic and extruded polyethylene and HAPEX™

	Modulus (GPa) Oscillating Pendulum	Modulus (GPa) Continuous Drive	Strength (MPa)
Isotropic Polyethylene	0.5	0.2	>20
Extruded Polyethylene	0.7		90
Isotropic HAPEX™		1.9	22
Extruded HAPEX™	2.3	2.5 (2.0–2.6)	50 (48–51) max

4. Discussion

4.1. Modulus and strength

The validity of the results for the flexural modulus at infinite span deserves special consideration. These results came from flexural tests performed on a single sample of extrudate, with a length of 250 mm. It was not possible to match exactly the strain rate at each span used, so the closest strain rate obtainable was used for the 150 mm and 100 mm spans. The sample was tested

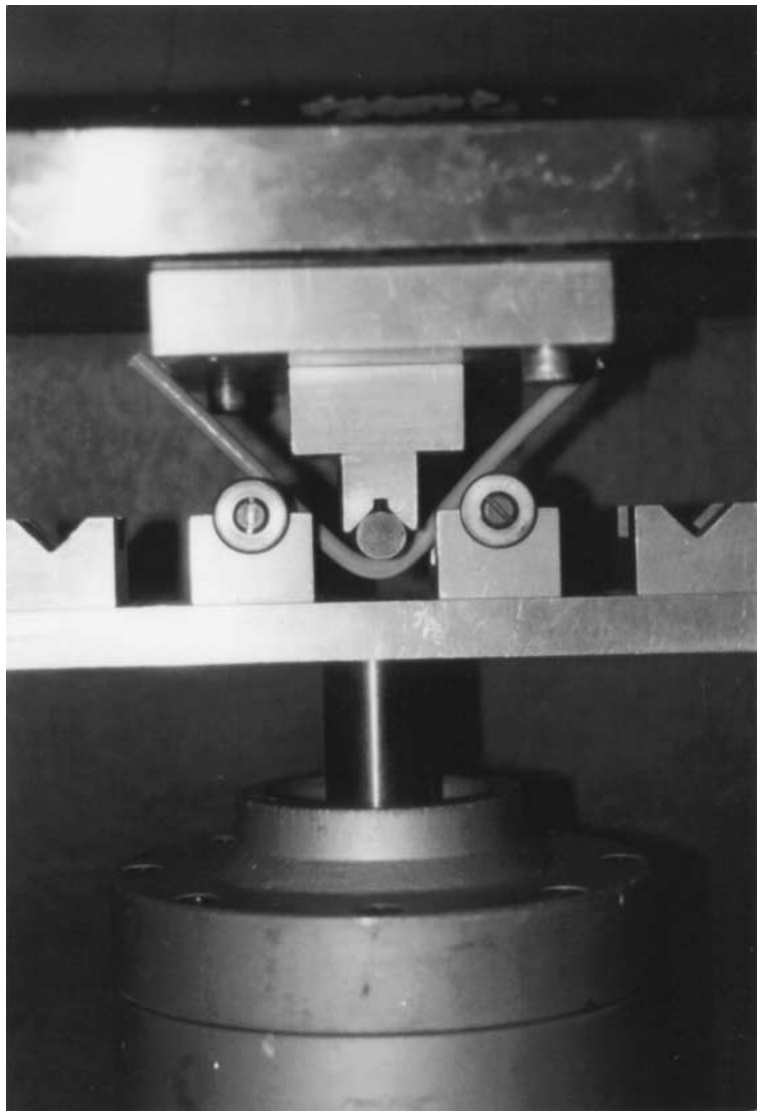

Figure 10 HAPEX^{TM} under flex test at large deformation.

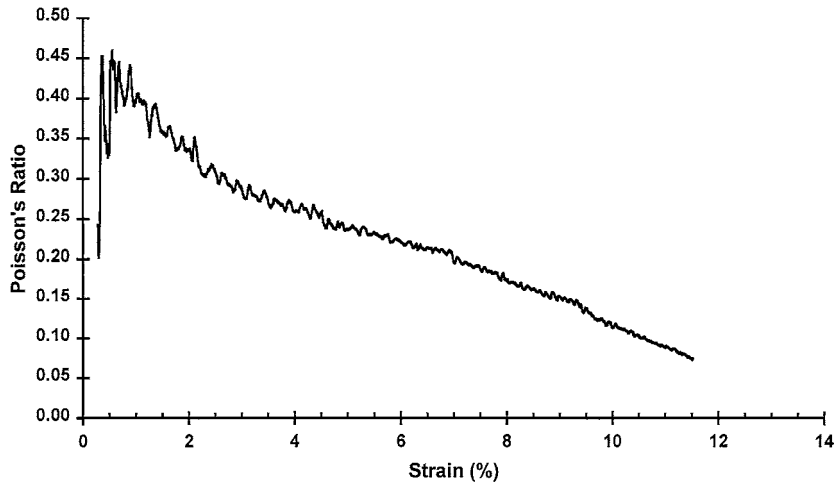

Figure 11 Poisson's ratio as a function of strain in extruded HAPEX^{TM}.

at 200 mm span first, and then shorter spans down to 50 mm. The results are shown in Fig. 13, which appear to show an anomalously low modulus at 150 mm span, possibly due to an unnoticed rotation of the cylindrical sample during the initial loading. Thus this point was discarded when extrapolating the curve back to the origin.

A further point that needs to be considered is the transverse tensile strength. Due to the relatively brittle nature of the material in this direction, significant care had to be taken when handling and machining the samples. Because of the nature of the test it was not possible to prepare waisted samples and all the samples failed at one of the grips. Several different gripping procedures

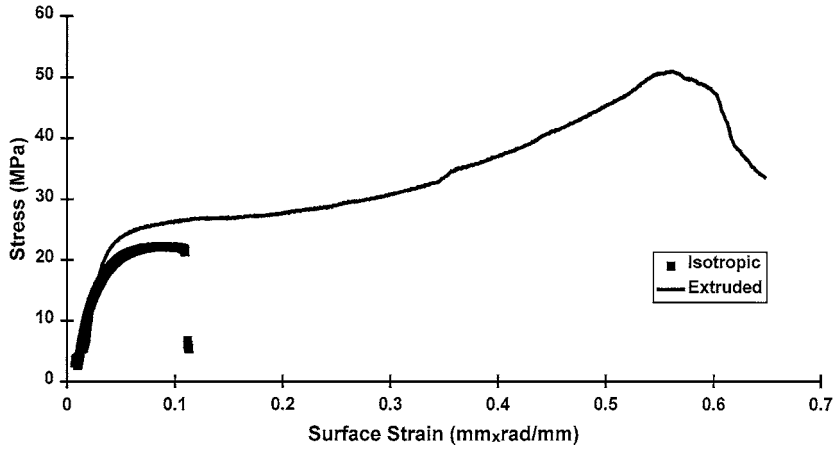

Figure 12 Sample Torsion Plots For Extruded And Isotropic HAPEX^{TM}.

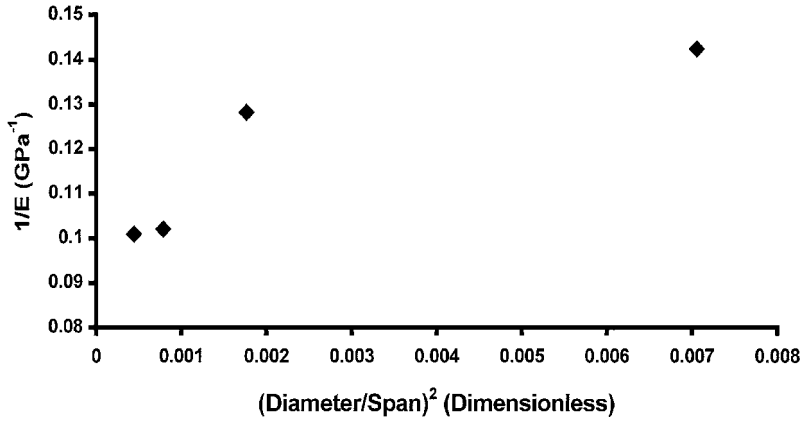

Figure 13 Plots showing determination of flexural modulus at infinite span.

were tried, but none appeared to alleviate the problem. Thus the transverse tensile strength quoted should be viewed more as a representative minimum value than an actual value and it would appear reasonable, given the comparison between other transverse values and the isotropic values to say that the isotropic tensile strength is a more representative measure of the actual transverse tensile strength.

4.2. Poisson's ratio

The Poisson's ratio is seen to change over the course of a test in the oriented materials. Fig. 11 shows the Poisson's ratio as a function of the axial strain developed in the material during a test. It can be seen that there is a steady decrease in the Poisson's ratio as the axial strain increases, and comparing with Fig. 9, this decrease in Poisson's ratio appears to begin at the same point as the stress-strain behaviour of the material becomes non linear, that is at around 0.5% strain. A decrease in Poisson's ratio, as seen here, normally indicates voiding occurring within the structure of the material. Density tests performed on the same sample before and after loading to approximately 7% strain have shown a density reduction of around 3%.

4.3. Torsion

The lower modulus value of the continuous drive method for the isotropic polyethylene is most likely a strain rate effect. The oscillating pendulum technique has a much higher effective strain rate, and it is well known that since isotropic polyethylene is a viscoelastic material, its properties are highly strain rate dependent.

As the samples have to be machined from 25 mm diameter extrudate, which is the most time consuming to produce, limited data are available, hence the mean and the range only are quoted. There are also limited data for the isotropic material, since only one torsion sample can be machined from an isotropic billet and each billet requires 1.5 days to manufacture. Thus if no range is quoted only one sample was tested.

4.4. Modelling

Although not presented here, attempts have been made to model the properties of the extruded composite using sophisticated finite element simulations [15]. These simulations show that the composite material is unexpectedly stiff in terms of considerations based on the elastic constants and volume fraction of the

TABLE V Summary of elastic constants for human femoral cortical bone (Refs 16–18)

$E_{parallel}$ (GPa)	17.0–27.4
$E_{transverse}$ (GPa)	11.5–18.8
$\nu_{parallel}$	0.19–0.31
$\nu_{transverse}$	0.31–0.58
G (GPa)	3.3–8.8

TABLE VI Comparison of properties for extruded HAPEX^{TM} and human femoral bone

	Mechanical		Ultrasonic		
			Human femur		
	Human femur [Ref 17]	Extruded HAPEX^{TM}	Ref 15	Ref 16	Extruded HAPEX^{TM}
$E_{parallel}$ (GPa)	17.0	10.3	27.4	20.0	16.3
$E_{transverse}$ (GPa)	11.5	5	18.8	12.0	9.0
$\nu_{parallel}$	0.31	0.43	0.19	0.22	0.33
$\nu_{transverse}$	0.58	0.4	0.31	0.38	0.42
G (GPa)	3.3	2.5	8.7	5.6	3.4

hydroxyapatite and the elastic constants predicted for oriented polyethylene of comparable deformation ratio. We are presently undertaking structural studies, principally by NMR, in an attempt to resolve this observation.

4.5. Comparison of elastic anisotropy of oriented HAPEX^{TM} and human and bovine cortical bone

There have been several detailed studies of the elastic anisotropy of cortical bone. Most determinations of the transverse elastic constants have been undertaken on the basis of ultrasonic measurements of wave velocity [16, 17]. Ashman *et al*. [17] claimed that there is a 1:1 correlation with traditional measurements at much lower strain rates, and this is confirmed by comparsion of the wave velocity measurements of Reilly and Burstein [18] at a strain rate of 0.1 s^{-1}. Table V shows the range of elastic constants for human femoral cortical bone, incorporating results for both ultrasonic measurements and lower strain rate measurements. Following the consensus of previous workers, it is assumed that there is transverse isotropy, i.e. any differences between the radial and circumferential directions in the bone can be neglected to a good approximation.

Comparsion of these data for human cortical bone and those obtained for HAPEX^{TM} (Table VI) show that the latter are much more sensitive to the test frequency, as would be expected for a composite partly composed of polyethylene which is a viscoelastic material where stiffness is sensitive to frequency. It is noteworthy that at ultrasonic frequencies [19], the elastic constants of oriented HAPEX^{TM}, are quite close to those of natural bone, and that the pattern of anisotropy $E_{\parallel} > E_{\perp} > G$ is very similar, also $\nu_{\perp} > \nu_{\parallel}$.

At the lower strain rates the elastic constants for the oriented HAPEX^{TM} are comparable to the lower range of properties in cortical bone. Consequently the hydrostatically extruded material is suitable for use in load bearing applications. In this respect it is important that the mechanical properties of the oriented HAPEX^{TM} are significantly increased in the extrusion direction over those of isotropic HAPEX^{TM} with little or no degradation of the properties in the direction perpendicular to the extrusion direction.

5. Conclusions

It has been demonstrated that it is possible to produce an extruded product of HAPEX^{TM} to a consistent standard with the high degree of reliability required for a commercial process.

TABLE VII Summary table of the principal elastic constants for polyethylene and HAPEX^{TM}

	Isotropic		Extruded	
	PE	HAPEX^{TM}	PE	HAPEX^{TM}
$E_{=}$	0.6	4.6	6.0	10.3
$E_{\perp}$	–	–		5
$\upsilon_{=}$	0.42	0.4	0.5	0.43
$\upsilon_{\perp}$	–	–	0.4	0.4
G	0.5	1.9	0.7	2.5

(E tensile modulus, υ Poisson's ratio, G torsional modulus, $=$ parallel to orientation direction, $\perp$ perpendicular to orientation direction).

A summary of the principal elastic constants for isotropic and extruded polyethylene and HAPEX^{TM} is shown in Table VII. A number of important points should be emphasised.

(1) The addition of hydroxyapatite to the polyethylene matrix results in a dramatic increase in the stiffness of the composite material.

(2) The mechanical properties of the hydrostatically extruded product are significantly increased in the extrusion direction, with little or no degradation of the properties in the direction perpendicular to the extrusion direction.

(3) The properties in the extrusion direction are increased to be in line with the lower range of properties found in cortical bone.

Acknowledgements

The IRC in Polymer Science and Technology and the IRC in Biomedical Materials were both funded by Core Grants from EPSRC. The authors also wish to thank Dr P. J. Hine of the IRC in Polymer Science and Technology for undertaking the ultrasonic measurements on the extruded HAPEX^{TM}, which will be reported fully in a separate publication.

References

1. W. BONFIELD, M. D. GRYNPAS, A. E. TULLY, J. BOWMAN and J. ABRAM, *Biomaterials* **2** (1981) 185.
2. W. BONFIELD, J. A. BOWMAN and M. D. GRYNPAS, UK Patent GB 2085461B (1984).
3. M. WANG, D. PORTER and W. BONFIELD, *Brit. Ceram. Trans.* **93** (1994) 91.
4. W. BONFIELD, *J. Biomed. Eng.* **10** (1988) 522.
5. R. N. DOWNES, S. VARDY, K. E. TANNER and W. BONFIELD, Bioceramics, in Proceedings of the 4th International Symposium on Ceramics in Medicine, edited by Bonfield, Hastings and Tanner (Butterworth-Heinemann, 1991) Vol. 4, p. 239.

6. J. L. DORNHOFFER, *Laryngoscope* **108** (1998) 531.
7. N. H. LADIZESKY, I. M. WARD and W. BONFIELD, *Polymers for Advanced Technologies* **8** (1997) 496.
8. I. M. WARD, W. BONFIELD and N. H. LADIZESKY, *Polymer International* **43** (1997) 333.
9. M. WANG, N. H. LADIZESKY, K. E. TANNER, I. M. WARD and W. BONFIELD, *J. Mater. Sci.* **35** (2000) 1023.
10. S. PATERSON, in "The Mechanical Behaviour of Materials Under Pressure," edited by H. L1. D. Pugh (Applied Science Publishers, 1971) p. 191.
11. S. SEIDO and S. MITSUGI, in "Hydrostatic Extrusion, Theory and Application," edited by N. Inoue and M. Nishihara (Elsevier Applied Science Ltd, London, 1985).
12. N. INOUE, in "Hydrostatic Extrusion, Theory and Application," edited by N. Inoue and M. Nishihara (Elsevier Applied Science Ltd, London, 1985).
13. R. A. DUCKETT, B. C. GOSWAMI, L. S. A. SMITH, I. M. WARD and A. M. ZIHLIF, *Brit. Polymer Journal* **10** (1978) 11.
14. A. A. GUSSEV, Private Communication, 1999.
15. H. S. YOON and J. L. KATZ, *J. Biomechanics* **9** (1976) 459.
16. R. B. ASHMAN, S. C. COWIN, W. C. VAN BUSKIRK and J. C. RICE, *ibid.* **17** (1984) 349.
17. D. T. REILLY and A. H. BURSTEIN, *ibid.* **8** (1975) 393.
18. M. BONNER, P. J. HINE and I. M. WARD, to be published.

Received 20 October 2000
and accepted 28 August 2001